Chemical Engineering Journal 149 (2009) 383–388

Contents lists available at ScienceDirect

Chemical Engineering Journal

journal homepage: www.elsevier.com/locate/cej

Modelling of laccase-catalyzed L-DOPA oxidation in a microreactor

Marina Tišma[a], Bruno Zelić[b], Đurđa Vasić-Rački[b], Polona Žnidaršič-Plazl[c], Igor Plazl[c,*]

[a] Josip Juraj Strossmayer University of Osijek, Faculty of Food Technology, F. Kuhača 18, HR-31000 Osijek, Croatia
[b] University of Zagreb, Faculty of Chemical Engineering and Technology, Savska c. 16, HR-10000 Zagreb, Croatia
[c] University of Ljubljana, Faculty of Chemistry and Chemical Technology, Aškerčeva 5, SI-1000 Ljubljana, Slovenia

ARTICLE INFO

Article history:
Received 19 June 2008
Received in revised form 9 January 2009
Accepted 20 January 2009

Keywords:
L-DOPA
Laccase
Oxidation
Microreactor
Reaction-diffusion dynamics
Modelling

ABSTRACT

Laccase-catalyzed L-DOPA oxidation in an oxygen-saturated water solution was studied in a y-shaped microreactor at different residence times. In a given microreactor geometry, up to 87% conversions of L-DOPA were achieved at residence times below 2 min. A two-dimensional mathematical model composed of convection, diffusion, and enzyme reaction terms was developed. Enzyme kinetics was described with the double substrate Michaelis–Menten equation, where kinetic parameters from previously performed batch experiments were used. Model simulations, obtained by a non-equidistant finite differences numerical solution of a complex equation system, were proved and verified in a set of experiments performed in a microreactor. Based on the developed model, further microreactor design and process optimization are feasible.

1. Introduction

Laccases (EC 1.10.3.2, *p*-diphenol: dioxygen oxidoreductases) are currently seen as very interesting enzymes for industrial oxidation reactions, since they are capable of oxidizing a wide variety of substrates [1–3]. Because enzymatic reactions offer several advantages over traditional chemical processes, they represent great potential for optimization of industrial processes, both economically and environmentally [4].

Microreaction technology is gaining importance in a broad range of areas, including chemistry and biochemistry. It is now clear that under the right conditions, microreactors can offer better selectivity, improved yields, increased process control, greater safety, faster scale-up, flexible production, and the opportunity to tap into previously avoided or novel chemistries. Due to the small amount of chemicals needed and high rate of heat and mass transfer, microreactors are also an extremely efficient tool for the rapid screening of (bio)catalysts [5,6].

Enzymatic microreactors, using either dissolved or immobilized enzymes, were principally developed in order to improve the routine work in biochemical analyses of proteomic and genetic material [7,8]. Although enzymatic microreactors have the potential for introduction into industrial-scale synthesis, not many patents have been developed in this field. The highest number of microreactor patents are in the field of organic chemistry (454 patents), while almost twice fewer patents exist in the fields of biochemistry, beer, spirits and wine technology, as well as microbiology (265 patents in total) [9].

Furthermore, mathematical modelling of enzymatic microreactors comprising flow distribution, transport phenomena and enzyme reaction kinetics, which would enable process description and optimization, has not been published up to date. A simplified model of *p*-chlorophenol degradation catalyzed by laccase, which was also the first report on the enzymatic reaction in a two-phase flow in a microchannel device, was reported by Maruyama et al. [10].

In order to better understand enzymatic oxidation processes in a microreactor, laccase-catalyzed 3,4-dihydroxy-L-phenylalanine (L-DOPA) oxidation was studied as a model process. L-DOPA is a representative of phenolic compounds with low solubility in water. It is a natural dietary amino acid, an intermediate in several metabolic pathways and a precursor of all catecholamine neurotransmitters and hormones, as well as of melanin [11]. The product of the first step of laccase-catalyzed L-DOPA oxidation is dopaquinon [12,13]. Quinons are highly reactive compounds which can polymerize spontaneously to form high molecular weight compounds such as melanin, or react with amino acids and proteins that enhance the brown colour produced in plants by the action of tyrosinase [14].

Laccase-catalyzed L-DOPA oxidation was studied in a microreactor with two inflows at different volumetric flow rates. A two-dimensional mathematical model, composed of convection, diffusion and enzyme reaction terms was developed.

* Corresponding author. Tel.: +386 1 2419 512; fax: +386 1 2419 530.
E-mail address: igor.plazl@fkkt.uni-lj.si (I. Plazl).

1385-8947/$ – see front matter © 2009 Elsevier B.V. All rights reserved.
doi:10.1016/j.cej.2009.01.025

Nomenclature

c	concentration, mol/m^3 (mM)
c_{O_2}	dissolved oxygen concentration, mol/m^3 (mM)
$D_{A/B}$	molecular diffusion coefficient, m^2/s
H	microchannel height, m
K_m^{LD}	Michaelis–Menten constant for L-DOPA, mol/m^3 (mM)
$K_m^{O_2}$	Michaelis–Menten constant for oxygen, mol/m^3 (mM)
L	microchannel length, m
P	pressure, kg/m s^2
t	time, s (min)
T	temperature, °C
V	volume, m^3 (μL)
V_m	maximal reaction rate, U/mg
$\bar{V}$	molar volume, m^3/mol
v_ξ	x-directional velocity of water, m/s
x	coordinate in the direction of channel length, m
y	coordinate in the direction of channel width, m
z	coordinate in the direction of channel height, m
W	microchannel half-width, m
X	conversion, %

Greek letters

Φ	total fluid flow rate, m^3/s (μL/min)
η	dynamic viscosity, kg/m s
τ	residence time, s
ξ	dimensionless independent variables, x/W
ψ	dimensionless independent variables, y/W
ω	dimensionless independent variables, z/W

Subscripts and abbreviations

E	enzyme (laccase)
i	inlet
L-DOPA	3,4-dihydroxy-L-phenylalanine
LD	L-DOPA
w	water

2. Theoretical background

2.1. Velocity profile in a microchannel

As stated in several literature reports, laminar flow characterizes microreactor flow conditions [5–10,15]. In order to simulate L-DOPA oxidation in a microreactor, the velocity profile was first set up.

As shown in Fig. 1a, the main microchannel was fed by two aqueous phase inflows: oxygen-saturated or half-saturated aqueous solution of laccase and oxygen-saturated or half-saturated aqueous solution of L-DOPA. Since both inflow phases had the same viscosity and were pumped in the system at the same flow rates, they both occupied the same fraction of the channel.

The assumption of the parabolic velocity profile, developed only in the smallest z-dimension, and therefore the uniform velocity profile in the y-direction was not possible due to the small width/height ratio of the microchannel used in our experiments, which was 4.4:1 (Fig. 1b). Therefore, a Poiseuille-type flow was developed considering the steady-state flow of aqueous phase and neglecting the compressibility and gravitational force (Eq. (1)):

$$0 = -\frac{\partial P}{\partial \xi} + \frac{\eta_w}{W}\left[\frac{\partial^2 v_\xi}{\partial \psi^2} + \frac{\partial^2 v_\xi}{\partial \omega^2}\right] \quad (1)$$

with the associated boundary conditions:

$$\begin{aligned} &v_\xi(\pm 1, \omega) = 0; \quad 0 \le \omega \le \frac{H}{W} \\ &v_\xi(\psi, 0) = 0; \quad -1 \le \psi \le 1 \\ &v_\xi\left(\psi, \frac{H}{W}\right) = 0; \quad -1 \le \psi \le 1 \end{aligned} \quad (2)$$

where dimensionless independent variables are defined as $\xi = x/W$, $\psi = y/W$, and $\omega = z/W$, and x, y and z are coordinates in the direction of channel length, width and height, respectively; H and W represent the height and half-width of the microchannel (m); v_ξ is the x-directional velocity of water (m/s) and η_w is the dynamic viscosity of water (kg/m s). A constant pressure gradient was applied along the length L of the microchannel, hence the term $\partial_\xi P(\xi)$ in Eq. (1) was simplified to $\Delta P/L$ [15].

2.2. Reaction-diffusion dynamics of laccase-catalyzed L-DOPA oxidation in a microchannel

For the description and prediction of microreactor performance, a 2D model was developed considering convection in the flow (x) direction and diffusion in two directions (x and y in Fig. 1). Dimensionless partial differential equations for steady-state conditions in the single pass microreactor system with the associated boundary conditions are as follows:
For L-DOPA (LD):

$$v_\xi(\psi)\frac{\partial c_{LD}}{\partial \xi} = \frac{D_{LD/w}}{W}\left[\frac{\partial^2 c_{LD}}{\partial \xi^2} + \frac{\partial^2 c_{LD}}{\partial \psi^2}\right] - \frac{WV_m c_E c_{LD}}{K_m^{LD} + c_{LD}} \frac{c_{O_2}}{K_m^{O_2} + c_{O_2}} \quad (3)$$

with the associated boundary conditions

$$\begin{aligned} &c_{LD}(0, \psi) = c_{i,LD}, \quad 1 \le \psi < 0 \\ &c_{LD}(0, \psi) = 0, \quad 0 \le \psi < 1 \\ &\frac{\partial c_{LD}}{\partial \xi}\left(\frac{L}{W}, \psi\right) = 0, \quad -1 \le \psi < 1 \\ &\frac{\partial c_{LD}}{\partial \psi}(\xi, \pm 1) = 0, \quad 0 \le \xi < \frac{L}{W} \end{aligned} \quad (4)$$

For oxygen (O_2):

$$v_\xi(\psi)\frac{\partial c_{O_2}}{\partial \xi} = \frac{D_{O_2/w}}{W}\left[\frac{\partial^2 c_{O_2}}{\partial \xi^2} + \frac{\partial^2 c_{O_2}}{\partial \psi^2}\right] - \frac{WV_m c_E c_{LD}}{K_m^{LD} + c_{LD}} \frac{c_{O_2}}{K_m^{O_2} + c_{O_2}} \quad (5)$$

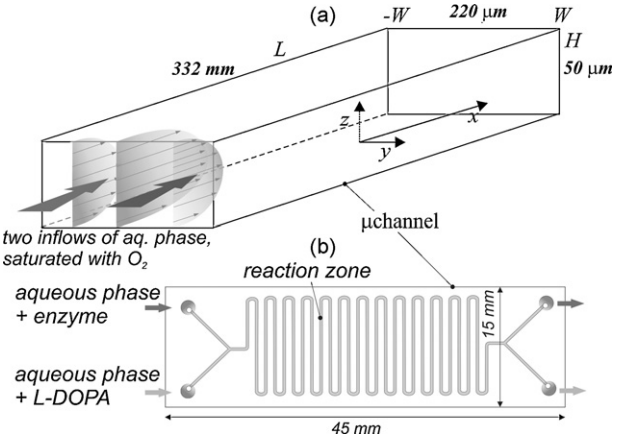

Fig. 1. Scheme of the microchannel ($2W$ = 220 μm, H = 50 μm and L = 332 mm).

with the associated boundary conditions

$$c_{O_2}(0,\psi) = c_{i,O_2}, \quad \frac{\partial c_{O_2}}{\partial \xi}\left(\frac{L}{W},\psi\right) = 0, \qquad -1 \le \psi < 1$$
$$\frac{\partial c_{O_2}}{\partial \psi}(\xi,\pm 1) = 0, \qquad 0 \le \xi < \frac{L}{W} \tag{6}$$

and for laccase (E):

$$v_\xi(\psi)\frac{\partial c_E}{\partial \xi} = \frac{D_{E/w}}{W}\left[\frac{\partial^2 c_E}{\partial \xi^2} + \frac{\partial^2 c_E}{\partial \psi^2}\right] \tag{7}$$

with the associated boundary conditions

$$c_E(0,\psi) = c_{i,E}, \quad 0 \le \psi < 1$$
$$c_E(0,\psi) = 0, \quad -1 \le \psi < 0$$
$$\frac{\partial c_E}{\partial \xi}\left(\frac{L}{W},\psi\right) = 0, \quad -1 \le \psi < 1 \tag{8}$$
$$\frac{\partial c_E}{\partial \psi}(\xi,\pm 1) = 0, \quad 0 \le \xi < \frac{L}{W}$$

where c_{LD}, c_{O_2} and c_E represent concentrations and $D_{LD/w}$, $D_{O_2/w}$ and $D_{E/w}$ represent diffusion coefficients for L-DOPA, oxygen and laccase in water, respectively; c_i denotes inlet concentrations, v_ξ is the x-directional velocity of water (m/s), V_m is maximal reaction rate, while K_m^{LD} and $K_m{}^{O_2}$ are Michaelis–Menten constants for L-DOPA and oxygen, respectively [16].

2.3. Estimation of diffusion coefficients

For the estimation of the molecular diffusion coefficient of L-DOPA in water ($D_{LD/w}$), the Scheibel empirical correlation was used [17]

$$D_{LD/w} = \frac{8.2\times 10^{-8} T}{\eta_w \bar{V}_{LD}^{1/3}}\left[1 + \left(\frac{3\bar{V}_w}{\bar{V}_{LD}}\right)\right]^{2/3} \tag{9}$$

where $\bar{V}_{LD}$ and $\bar{V}_w$ (m^3/mol) are molar volumes of L-DOPA and water, respectively, η_w is water dynamic viscosity (kg/m s) and T is temperature (K). For the estimation of the molecular diffusion coefficient of oxygen in water $D_{O_2/w}$ we used the Stokes–Einstein equation [18]

$$D_{O_2/w} = 6.92\times 10^{-10}\left(\frac{T}{\eta_w}\right) \tag{10}$$

while the molecular diffusion coefficient of laccase in water ($D_{E/w}$) was taken from the literature [19].

3. Numerical analysis

Finite differences on the 2D Cartesian grid were used to replace the partial derivatives in the presented model equations. Static equidistant finite differences were transformed to non-equidistant finite differences. In order to solve the complex non-linear system of model equations, *Mathematica 5.2* code was developed, which enabled fast converging to the solution [15].

4. Experimental

4.1. Materials

4.1.1. Chemicals

L-DOPA and $(NH_4)_2SO_4$ were from Fluka A.G. (Steinheim, Germany), Na_2HPO_4, KH_2PO_4 and perchloric acid were from Merck (Darmstadt, Germany) and HCl was purchased from Kemika (Zagreb, Croatia).

4.1.2. Enzyme

Laccase from *Trametes versicolor* was purchased from Fluka A.G. (Buchs, Switzerland).

4.2. Methods

4.2.1. Laccase-catalyzed L-DOPA oxidation in a microreactor

Laccase-catalyzed L-DOPA oxidations were carried out in glass microreactors with the y-shaped inflow and outflow channels and with the main channel with dimensions: 220 μm width, 50 μm height and 332 mm length (Micronit Microfluidics B.V., Enschede, The Netherlands). Oxygen-saturated ($c_{i,O_2} = 1.15$ mM) or half-saturated ($c_{i,O_2} = 0.58$ mM) L-DOPA solution in 0.2 mol/L phosphate buffer (pH 5.4) were fed from one inflow and oxygen-saturated or half-saturated laccase solution in 0.2 mol/L phosphate buffer (pH 5.4) were fed from another inflow of the y-shaped microreactor (Fig. 1). Different concentrations of L-DOPA were used at the inlet: $c_{i,LD} = 0.5$, 3 or 5 mM, while enzyme concentration at the inlet was kept constant $c_{i,E} = 0.2$ mg/mL. Two syringe pumps (PHD 4400 Syringe Pump Series, Harvard Apparatus, Holliston, USA) were used for solution supply. Both solutions were pumped in at equal and constant flow rates of 100, 10, 5 or 1 μL/min, so that the total flow rates in the microreactor were 200, 20, 10 or 2 μL/min. The samples from the microreactor were diluted in 0.1 mol/L HCl before the HPLC analysis.

4.2.2. Analytics

The concentration of L-DOPA in samples from microreactor, diluted in 0.1 mol/L HCl, was evaluated by HPLC (Knauer, Berlin, Germany) at 30 °C with a reverse phase C_{18} 125 mm × 4 mm × 5 μm column (LiChrospher® 100, Merck, Darmstadt, Germany), and UV detection at 280 nm. The mobile phase used was water with the addition of perchloric acid until pH 2.10–2.15 was reached and sample elution was performed at the flow rate of 0.7 mL/min [16]. L-DOPA standards for the calibration curve and samples taken from the reactor were diluted with hydrochloric acid (0.1 mol/L). Retention time of L-DOPA was 7.3 min.

An oxymeter (WTW pH/Oxi 340, electrode WTW Cellox 325, Weinheim, Germany) was used to measure dissolved oxygen concentration in the reaction media.

5. Results and discussion

5.1. Fluid flow in a microchannel

In order to observe a fluid flow within the microchannel device, plain water and coloured water were fed through separate inflows

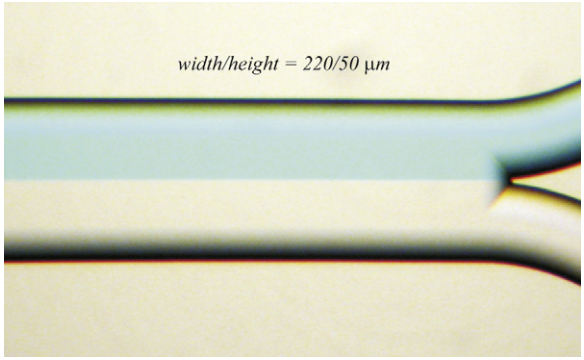

Fig. 2. Microscopic observation of a flow pattern of water and coloured water, entering through separate inflow channels at equal flow rates of 100 μL/min (total flow rate through the main microchannel Φ = 200 μL/min). (For interpretation of the references to colour in this figure legend, the reader is referred to the web version of the article.)

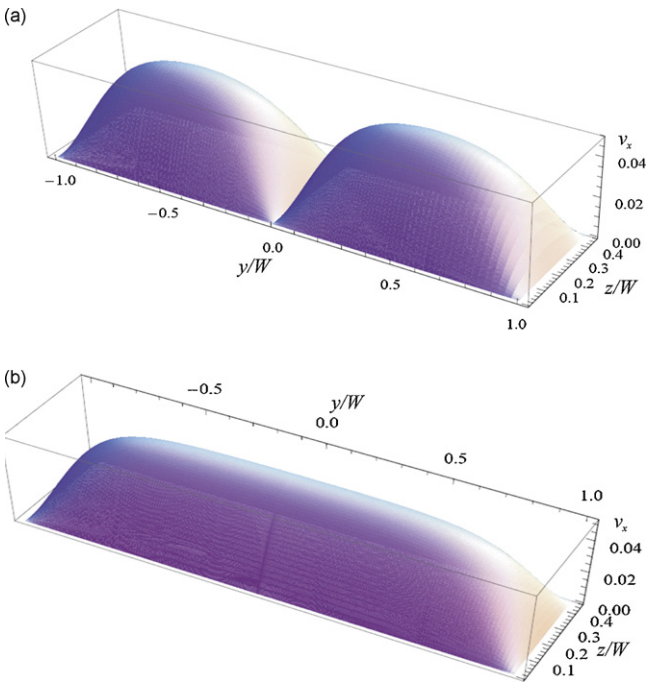

Fig. 3. A mathematical model simulation of a velocity profile at the flow rate of each inflow fluid of 20 μL/min: (a) at the microchannel inlet and (b) a developed profile in the microchannel immediately after the entrance.

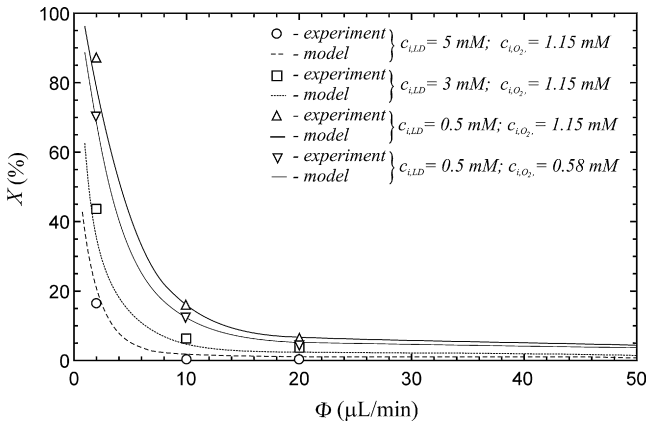

Fig. 4. Enzymatic oxidation of L-DOPA—experimental data and the results of mathematical model calculations of conversion based on average dimensionless L-DOPA concentration at the outlet of the microchannel at different total fluid flow velocities through the main channel (L = 332 mm).

at the same flow rates. Microscopic observations, presented in Fig. 2, confirmed the laminar flow parallel to the sidewalls of the channels for the flow rates used in our studies (bellow 200 μL/min). Furthermore, the position of the interface was exactly in the middle of the channel, which again confirmed our assumptions for the model (Fig. 2).

The results of the 2D numerical simulation of a fluid flow in the microchannel with the position of the interface area in the middle of the channel, using model Eqs. (1) and (2), revealed that at steady-state conditions, a fully developed profile takes place very shortly after the beginning of the microchannel (Fig. 3). This enabled us to consider a fully developed velocity profile, presented in Fig. 3b, in further simulations of concentration profiles within the whole microchannel.

5.2. Estimation of model parameters

Diffusion coefficients of L-DOPA and oxygen in water at 25 °C were calculated according to Eqs. (9) and (10). They were $D_{LD/w} = 0.436 \times 10^{-9}$ m^2/s and $D_{O_2/w} = 2.31 \times 10^{-9}$ m^2/s, while diffusion coefficients of laccase in water $D_{E/w} = 3.6 \times 10^{-11}$ m^2/s was taken from the literature [19]. Kinetic parameters of laccase-catalyzed L-DOPA oxidation, previously estimated in a batch reactor [16], were used for mathematical modelling of enzyme reaction within the microchannel: V_m = 6.897 U/mg, $K_m^{LD} = 0.469$ mM and $K_m{}^{O_2} = 0.099$ mM.

5.3. Enzyme reaction in a microchannel

The results of the experiments of laccase-catalyzed L-DOPA oxidations, at steady-state conditions in a microreactor, performed with different inlet L-DOPA and oxygen concentrations and at different fluid flow rates, are summarized in Table 1. Up to 87% conversion of L-DOPA was reached with the lowest inlet L-DOPA concentration of 0.5 mM in oxygen-saturated medium (c_{i,O_2} = 1.15 mM) and at the longest residence time of 110 s (total fluid flow rate Φ = 2 μL/min). As expected, at higher L-DOPA concentrations ($c_{i,LD}$ = 3 or 5 mM) in oxygen-saturated medium and at higher flow rates and thereby shorter residence times, adequately lower conversions were obtained in the chosen microreactor. Noticeable lower conversions were observed at half lower oxygen concentration ($c_{i,O_2} = 0.58$ mM) as compared to oxygen-saturated 0.5 mM L-DOPA solutions, which confirms the influence of oxygen on biotransformation rate. At the highest fluid flow rate tested (Φ = 200 μL/min, τ = 1.1 s), we did not observe any conversion within the microchannel for any of the tested reaction conditions. Furthermore, no biotransformation occurred at residence times up to 22 s when using the highest concentrations of both substrates.

The comparison with the results from the ideally mixed semi-batch reactor with continuous aeration confirmed an advantage of microreactor technology over classical reactors, where the same 87% conversion of L-DOPA (initial conc. 0.5 mM) was reached after 4 min. However, such high conversion rates were achieved only at the continuous supply of pure oxygen in a well agitated and intensively sparged laboratory-scale vessel (beaker), providing optimal mass transport [16]. Furthermore, continuous process operation with immobilized enzyme would even improve process economics in integrated microstructured devices.

In order to analyse the experimental results and to predict microreactor performance, mathematical model simulations were performed using Eqs. (3)–(8), considering the fully developed velocity profile within the whole microchannel, shown in Fig. 3b,

Table 1
Experimental results of L-DOPA conversion at different residence times and for different inlet L-DOPA and oxygen concentrations. Results are the average of at least three experiments with relative error below 12%.

Φ (μL/min)	τ (s)	X (%)			
		$c_{i,LD}$ = 5 mM, c_{i,O_2} = 1.15 mM	$c_{i,LD}$ = 3 mM, c_{i,O_2} = 1.15 mM	$c_{i,LD}$ = 0.5 mM, c_{i,O_2} = 1.15 mM	$c_{i,LD}$ = 0.5 mM, c_{i,O_2} = 0.58 mM
200	1.1	0	0	0	0
20	11	0	3.5	6.7	4.9
10	22	0	6.1	16	15.3
2	110	16.4	43.4	87	71

and the laminar nature of microfluidic flow. The comparison of the results of mathematical model simulations, based on kinetic parameters previously determined in batch experiments [16] with experimental data is presented in Fig. 4. As can be seen, the experimental conversions of L-DOPA performed in a microreactor are in good agreement with the model predictions for all inlet L-DOPA and oxygen concentrations and for all applied flow rates.

5.4. Concentration profiles within the microchannel

Concentration profiles of a particular component within the main microchannel were obtained by a numerical solution of the non-linear system of partial differential equations based on the previously described velocity profile and double substrate Michaelis–Menten kinetic model (Eqs. (1)–(10)). The results for L-DOPA, oxygen and enzyme concentrations along the microreactor with inlet L-DOPA concentration of 0.5 mM in oxygen-saturated aqueous solution at the lowest tested total flow rate of 2 μL/min are presented in Fig. 5. As evident from Fig. 5a, the phenolic substrate readily diffused into the other half of aqueous solution and was evenly distributed through the whole microchannel at approximately one third of the channel length. A decrease in L-DOPA concentration due to the enzymatic reaction along the microchannel is also evident from Fig. 5a. Oxygen as the second substrate for oxidation was supplied at both inlets with the same concentration ($c_{i,O_2} = 1.15$ mM) and was consumed along the microchannel (Fig. 5b). As seen from both figures, L-DOPA was almost depleted along the channel, while oxygen was present in redundance. The reason for the fact that both reactants did not completely react at these operational conditions is presumably the low molecular diffusivity of laccase in water and short residence times, preventing the enzyme to diffuse completely into the other part of aqueous solution, as evident from the simulation of the laccase concentration profile along the microchannel in Fig. 5c. The same explanation could be used also for the explanation of poor results of L-DOPA oxidation at higher inlet concentration and at shorter residence times, suggesting the use of longer or consecutively bounded microreactors.

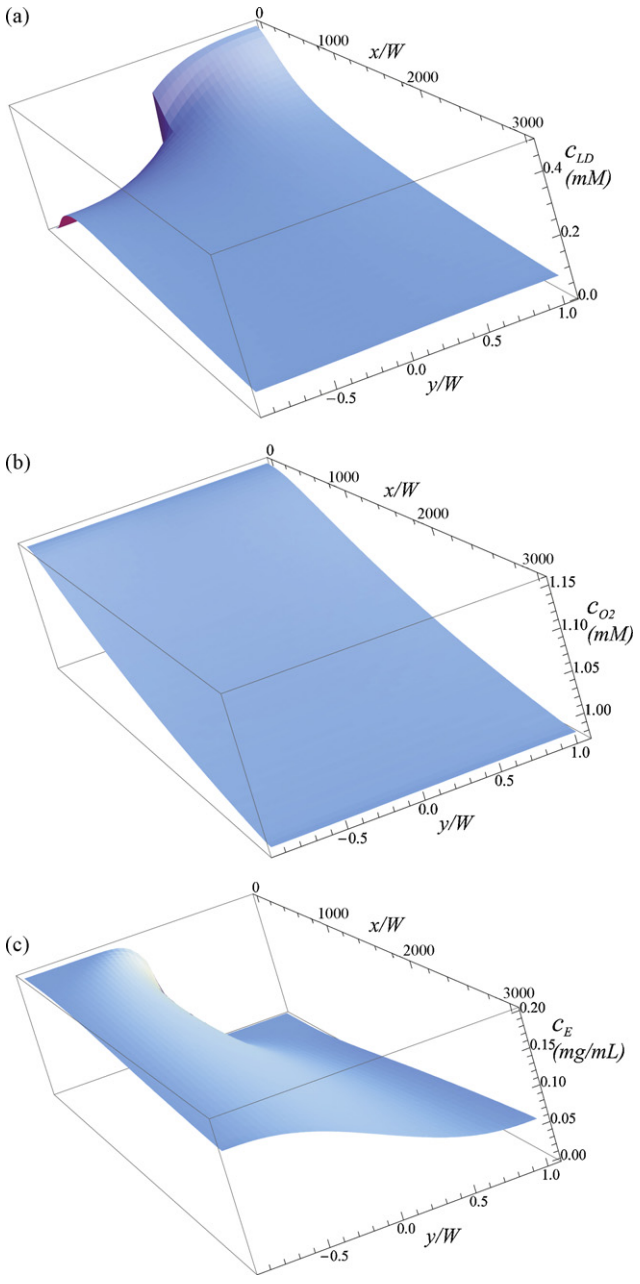

Fig. 5. Mathematical simulations of concentration profiles of (a) L-DOPA, (b) oxygen and (c) laccase along the main microchannel ($L = 332$ mm) with inlet L-DOPA concentration of 0.5 mM at total flow rate of 2 μL/min ($c_{i,LD} = 0.5$ mM, $c_{i,O_2} = 1.15$ mM and $c_{i,E} = 0.2$ mg/mL).

6. Conclusion

In the present paper L-DOPA oxidation catalyzed by laccase from *T. versicolor* was performed in the microreactor. High conversion of 87% was reached for 0.5 mM of L-DOPA at a residence time of 100 s. For higher inlet concentration of this substrate, the oxidation in the same microreactor was less efficient at the same operational conditions, partly due to the low molecular diffusivity of laccase in water and thereby insufficient enzyme concentration in some parts of the channel, suggesting use of a longer microchannel. Based on the developed model simulations, which were in good agreement with experimental data, and enzyme immobilization, further microreactor design and process optimization are feasible.

References

[1] A.M. Mayer, R.C. Staples, Laccase: new function for an old enzyme, Phytochemistry 60 (2002) 551–565.
[2] S.G. Burton, Laccases and phenol oxidases in organic syntheses—a review, Curr. Org. Chem. 7 (2003) 1317–1331.
[3] S. Rodrígues Cuoto, J.L. Toca Herrera, Industrial and biotechnological applications of laccases: a review, Biotechnol. Adv. 24 (2006) 500–513.
[4] Đ. Vasić-Rački, History of industrial biotransformation—dreams and realities, in: A. Liese, K. Seelbach, C. Wandrey (Eds.), Industrial Biotransformation, Wiley–VCH, Weinheim, 2006, pp. 1–36.
[5] W. Ehrfeld, V. Hessel, H. Löwe, Microreactors, Wiley–VCH, Weinheim, 2000.
[6] A.M. Thayer, Harnessing microreactions, Chem. Eng. News 83 (22) (2005) 43–52.
[7] M. Miyazaki, H. Maeda, Microchannel enzyme reactors and their application for processing, Trends Biotechnol. 24 (2006) 463–470.
[8] P.L. Urban, D.M. Goodall, N.C. Bruce, Enzymatic microreactors in chemical analysis and kinetic studies, Biotechnol. Adv. 24 (2006) 42–57.
[9] V. Hessel, C. Knobloch, H. Löwe, Review on patents in microreactor and micro process engineering, Recent Patent Chem. Eng. 1 (2008) 1–16.
[10] T. Maruyama, J. Uchida, T. Ohkawa, T. Futami, K. Kotayama, K. Nishizawa, K. Sotowa, F. Kubota, N. Kamiya, M. Goto, Enzymatic degradation of p-chlorophenol in a two-phase flow microchannel system, Lab Chip 3 (2003) 308–312.
[11] V. Bonifati, G. Meco, New, selective catechol-O-methyltransferase inhibitors as therapeutic agents in Parkinson's disease, Pharmacol. Therapeut. 81 (1999) 1–36.
[12] P.R. Williamson, Laccase and melanin in the pathogenesis of *Cryptococcus neoformans*, Front Biosci. 2 (1997) 99–107.
[13] P.R. Williamson, K. Wakamatsu, S. Ito, Melanin biosynthesis in *Cryptococcus neoformans*, J. Bacteriol. 180 (1998) 1570–1572.
[14] Q.X. Chen, X.D. Liu, H. Huang, Inactivation kinetics of mushroom tyrosinase in the dimethyl sulfoxide solution, Biochemistry (Moscow) 68 (2003) 644–649.

[15] P. Žnidaršič-Plazl, I. Plazl, Steroid extraction in a microchannel system—mathematical modelling and experiments, Lab Chip 7 (2007) 883–889.
[16] M. Tišma, P. Žnidaršič-Plazl, I. Plazl, B. Zelić, Đ. Vasić-Rački, Modelling of L-DOPA oxidation catalyzed by laccase, Chem. Biochem. Eng. Q. 22 (3) (2008) 307–313.
[17] J. Li, P.W. Carr, Accuracy of empirical correlations for estimating diffusion coefficients in aqueous organic mixtures, Anal. Chem. 69 (1997) 2530–2536.
[18] C.E. St-Denis, C.J.D. Fell, Diffusivity of oxygen in water, Can. J. Chem. Eng. 49 (1971) 885.
[19] S. Shleev, A. Christenson, V. Serezhenkov, D. Burbaev, A. Yaropolov, L. Gorton, T. Ruzgas, Electrochemical redox transformations of T1 and T2 copper sites in native *Trametes hirsuta* laccase at gold electrode, Biochem. J. 385 (2005) 745–754.